Electronic Supplementary Material (ESI) for Nanoscale.

Supporting Information for

Strongly coupled hybrid nanostructures for selective hydrogen detection – understanding the role of noble metals in reducing cross-sensitivity

Bin Liu,[a] Daoping Cai,[b] Yuan Liu,[a] Dandan Wang,[a] Lingling Wang,[a] Wuyuan Xie,[c] Qiuhong Li*[a] and Taihong Wang *[a]

[a] *Pen-Tung Sah Institute of Micro-Nano Science and Technology of Xiamen University, Xiamen, 361005, China.*

[b] *Department of Chemistry, College of Chemistry and Chemical Engineering, Xiamen University, Xiamen, 361005, China*

[c] *Department of Physics, School of Physics and Mechanical & Electrical Engineering, Xiamen University, Xiamen, 361005, China*

Corresponding author: Qiuhong Li, *Email: liqiuhong2004@hotmail.com*; Taihong Wang, *Email: thwang@xmu.edu.cn*

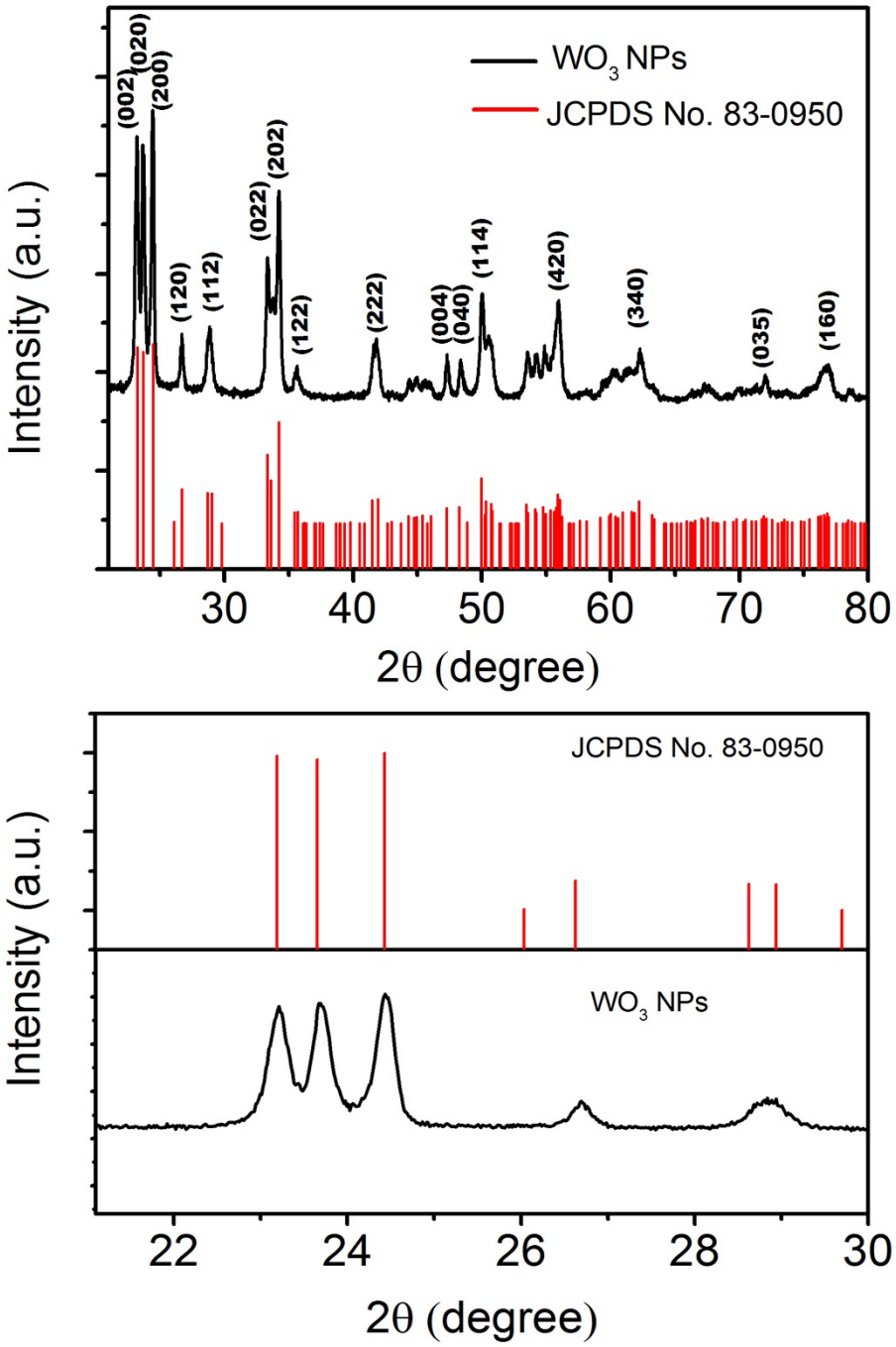

Fig. S1 (a) XRD pattern of the WO_3 NPs. (b) Detailed peak position comparison of the WO_3 NPs with the reference pattern taken from JCPDS No. 83-0950.[1]

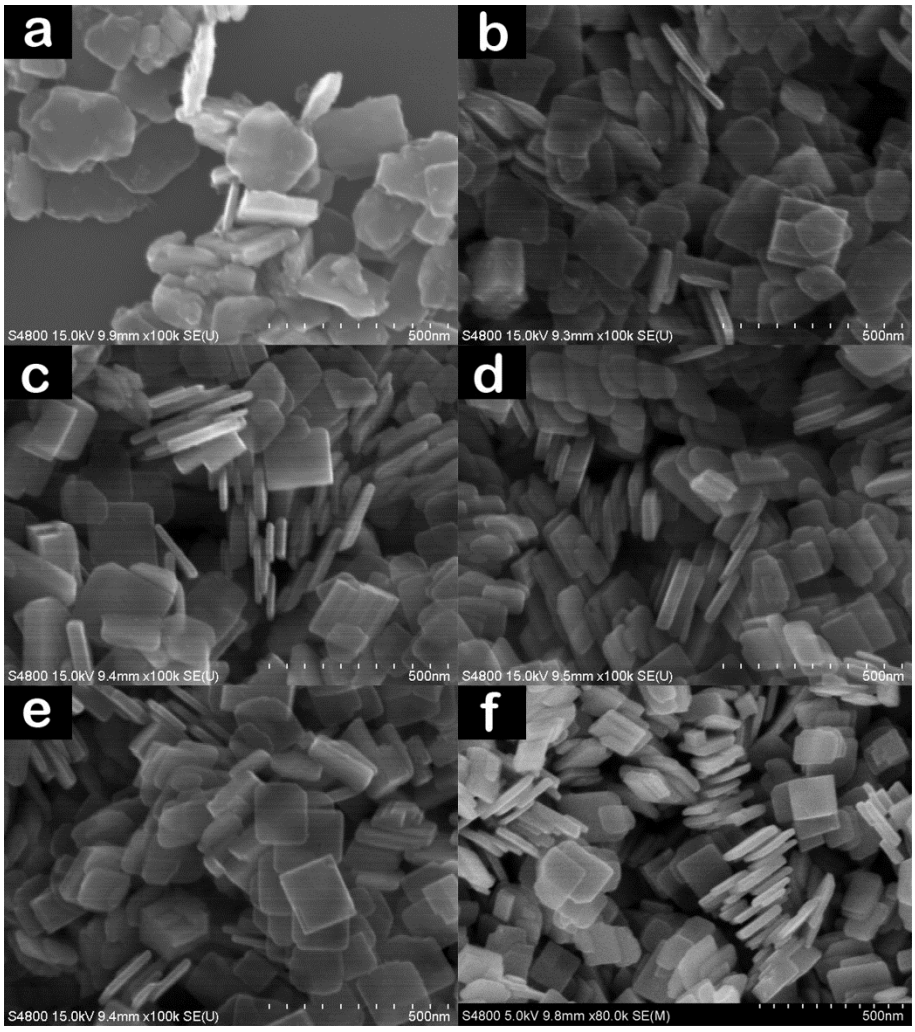

Fig. S2 SEM images of the WO_3 NPs synthesized by adding different amount of hydrochloric acid: (a) 0.1 mL, (b) 0.2 mL, (c) 0.4 mL, (d) 0.6 mL, (e) 0.8 mL and (f) 1.0 mL.

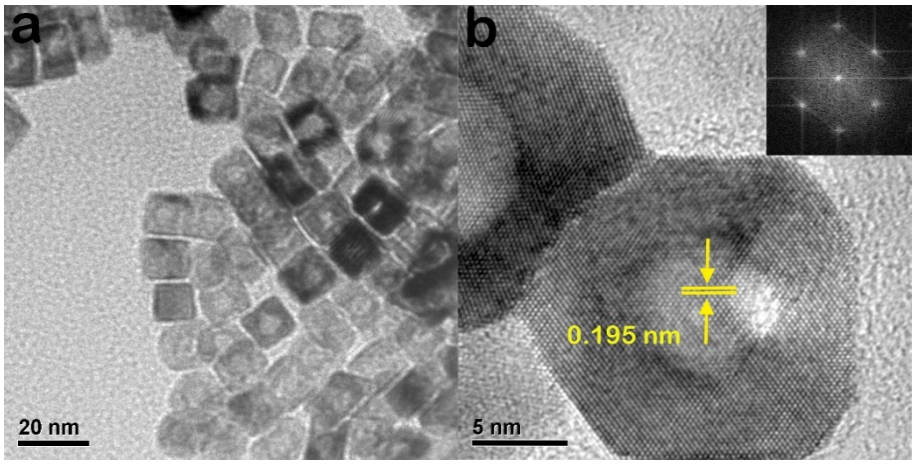

Fig. S3 TEM (a) and high resolution TEM (b) images of the Pt/Pd bimetallic nanocubes.

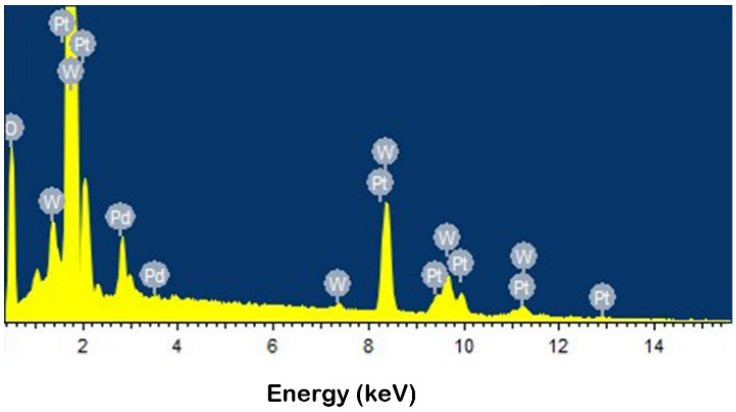

Quantification Results

Element	Weight %	Atomic %
W	65.64	21.59
O	19.08	72.13
Pt	9.31	2.89
Pd	5.96	3.39

Fig. S4 EDX spectrum and the quantification analysis results of the Pt/Pd-WO_3 hybrid nanostructures.

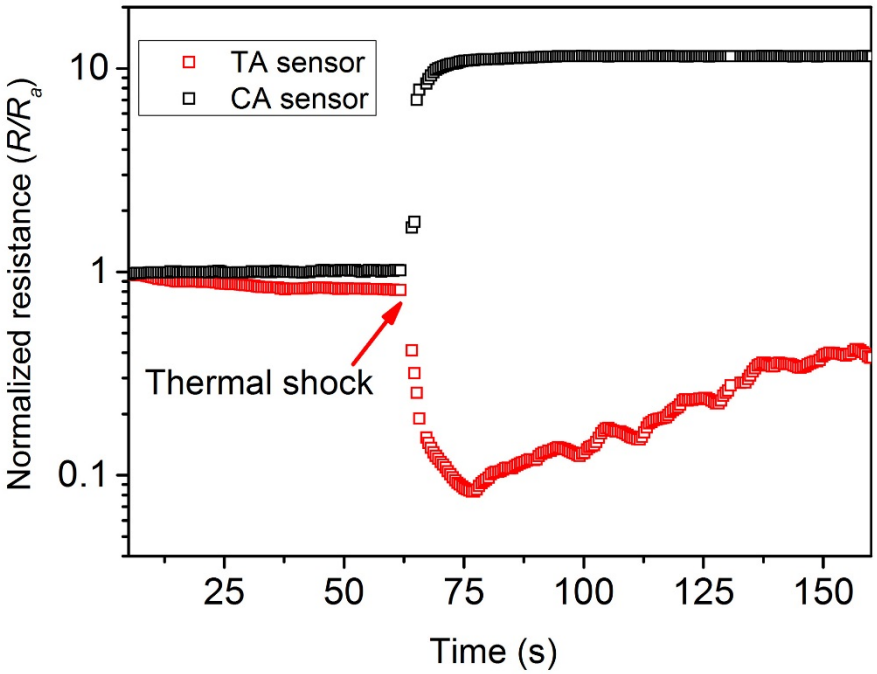

Fig. S5 The resistance change of the TA and CA sensor under a thermal shock (rapid heating from room temperature to 80℃). The slight decrease in the resistance of the TA sensor in the first minute is most probably caused by the self-heating effect.[2]

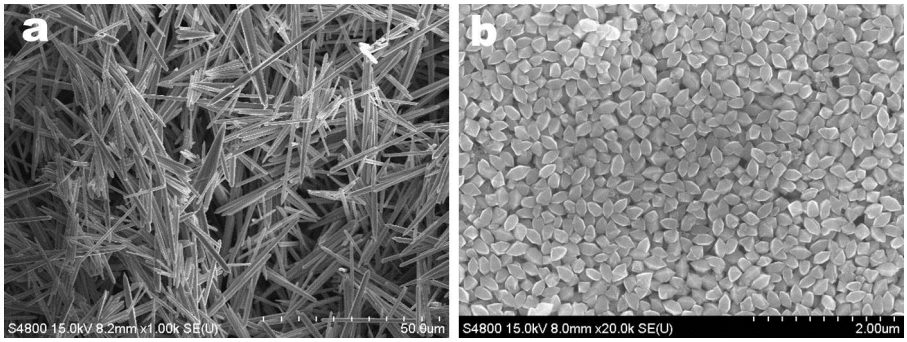

Fig. S6 SEM images of the ZnO columns and SnO_2 octahedrons synthesized according to Ref. S3 and Ref. S4, respectively.

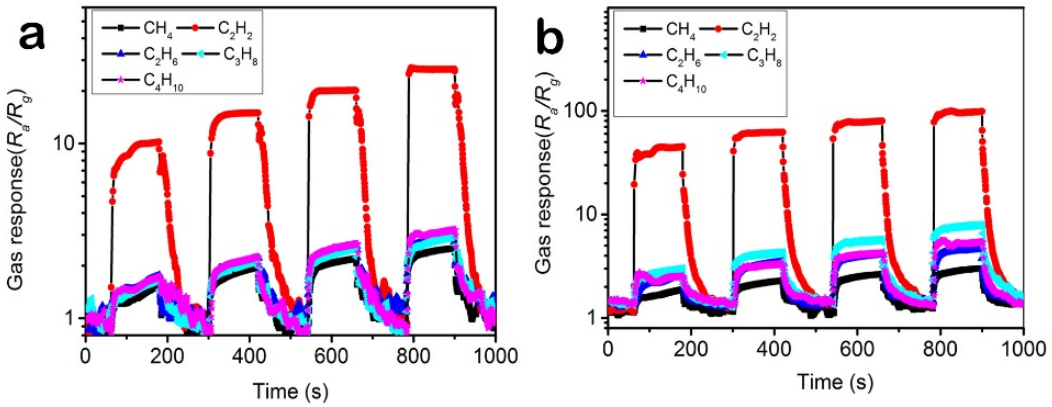

Fig. S7 Transient responses of the TA sensors made from ZnO (a) and SnO_2 (b) to different hydrocarbon gases.

Gas	Structure	HOMO (eV)	R_WO_3	R_ZnO	R_SnO_2
CH_4	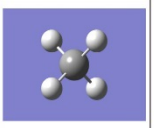	-12.5	5.5	2.1	2.23
C_2H_2	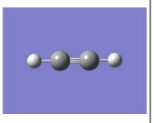	-9.8	12.1	20.1	77.7
C_2H_6	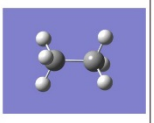	-11.1	5.8	2.4	3.9
C_3H_8	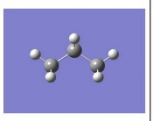	-10.6	5.7	2.4	5.5
C_4H_{10}	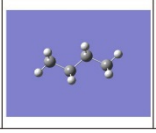	-10. 4	5.6	2.5	4.1

Table S1 Summary of the molecular structures, HOMO energy levels and responses of the three TA sensors to different hydrocarbon gases with a concentration of 0.1 vol%.

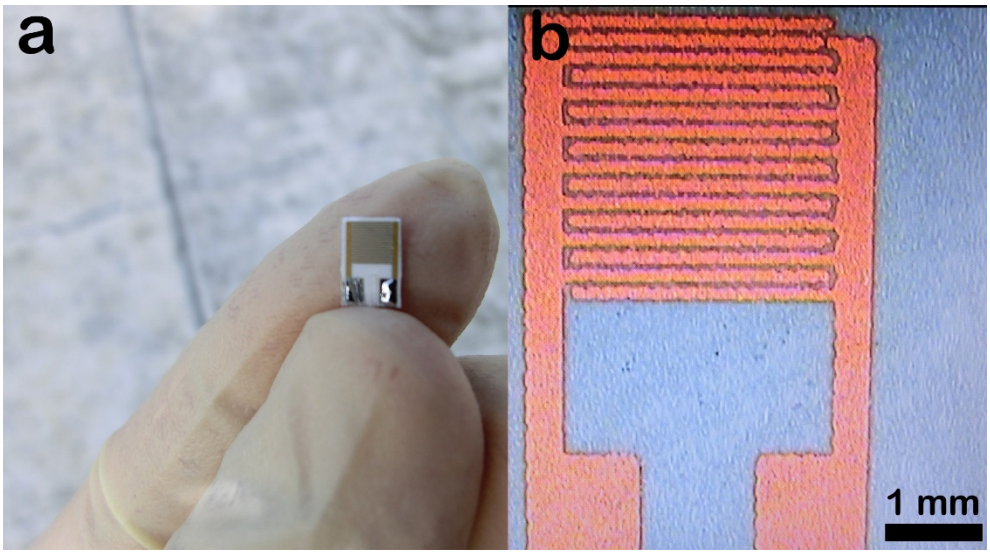

Fig. S8 Optical images of the device, showing the dimensions of the sensor.

1. P. M. Woodward, A. W. Sleight and T. Vogt, *J Phys Chem Solids*, 1995, 56, 1305-1315.

2. E. Strelcov, S. Dmitriev, B. Button, J. Cothren, V. Sysoev and A. Kolmakov, *Nanotechnology*, 2008, 19. 355502

3. Xi-Guang Han, Hui-Zhong He, Qin Kuang,* Xi Zhou, Xian-Hua Zhang, Tao Xu, Zhao-Xiong Xie,*

Lan-Sun Zheng, *J. Phys. Chem. C*, 2009, 113, 584.
4. X.G. Han, M.S. Jin, S.F. Xie, Q. Kuang,* Z.Y. Jiang, Y.Q. Jiang, Z.X. Xie,* L.S. Zheng, Angew. Chem. Int. Ed., 2009, 48, 9180-9183.